

# PROCEEDINGS OF SPIE

[SPIDigitalLibrary.org/conference-proceedings-of-spie](https://spiedigitallibrary.org/conference-proceedings-of-spie)

## Extrasolar planet science with the Antarctic planet interferometer

James P. Lloyd, Benjamin F. Lane, Mark R. Swain, John W.V. Storey, Tony Travouillon, et al.

James P. Lloyd, Benjamin F. Lane, Mark R. Swain, John W.V. Storey, Tony Travouillon, Wesley A. Traub, Christopher K. Walker, "Extrasolar planet science with the Antarctic planet interferometer," Proc. SPIE 5170, Techniques and Instrumentation for Detection of Exoplanets, (19 November 2003); doi: 10.1117/12.506895

**SPIE.**

Event: Optical Science and Technology, SPIE's 48th Annual Meeting, 2003, San Diego, California, United States

# Extrasolar Planet Science with the Antarctic Planet Interferometer

James P. Lloyd<sup>a</sup>, Ben F. Lane<sup>a</sup>, Mark R. Swain<sup>b</sup>, John W. Storey<sup>c</sup>, Tony Travouillon<sup>c</sup>,  
Wesley A. Traub<sup>d</sup> and Chris K. Walker<sup>e</sup>

<sup>a</sup>California Institute of Technology, Pasadena, CA 91125 USA

<sup>b</sup>Jet Propulsion Laboratory, Pasadena, CA 91109 USA

<sup>c</sup>School of Physics, University of New South Wales, Sydney, Australia

<sup>d</sup>Smithsonian Astrophysical Observatory, Cambridge, MA 02138 USA

<sup>e</sup>University of Arizona, Steward Observatory, Tucson, AZ 85721

## ABSTRACT

The primary limitation to ground based astronomy is the Earth's atmosphere. The atmosphere above the Antarctic plateau is fundamentally different in many regards compared to the atmosphere at temperate sites. The extreme altitude, cold and low humidity offer a uniquely transparent atmosphere at many wavelengths. Studies at the South Pole have shown additionally that the turbulence properties of the night time polar atmosphere are unlike any mid latitude sites. Despite relatively strong ground layer turbulence, the lack of high altitude turbulence combined with low wind speeds presents favorable conditions for interferometry. The unique properties of the polar atmosphere can be exploited for Extrasolar Planet studies with differential astrometry, differential phase and nulling interferometers. This paper combines the available data on the properties of the atmosphere at the South Pole and other Antarctic plateau sites for Extrasolar Planet science with interferometry.

**Keywords:** Atmospheric Turbulence, Extrasolar Planets, Interferometry

## 1. INTRODUCTION

The amplitude and phase corruption of electromagnetic radiation by the atmosphere sets the limits for ground based astronomical observations. The quality of astronomical observations is advanced not only by improvements in the instruments themselves, but by deployment at the best possible sites. Atmospheric transparency, background and seeing (indicated by the full width of the point spread function at half maximum, FWHM) are the parameters by which sites are typically compared. For observations in the optical and near infrared, high mountain sites that are above most of the Earth's boundary layer such as Mauna Kea and the Chilean Andes are superior because of favorable values of these parameters. Transparency and background are parameters that are relatively simple to quantify and interpret. However, there is much more to seeing than the FWHM of images taken through the turbulent atmosphere. It has long been recognized that the turbulence properties of the antarctic atmosphere may offer fundamentally different seeing (turbulence) properties than mid latitude sites.<sup>1</sup>

As part of the site characterization program of the Center for Astrophysical Research in Antarctica (CARA), a program was undertaken to measure the seeing at the South Pole with optical methods. The results indicated relatively poor seeing by the standard metric of image quality.<sup>2</sup> Marks *et al.*(1996, 1999)<sup>3,4</sup> also measured the  $C_N^2$  profile at the South Pole with tower and balloon based microthermal sensors. These profiles clearly shows that the vast majority of the turbulence is at altitudes below 1 km. In light of the importance of a comprehensive understanding the site statistics, an ongoing site testing program involving the South Pole and remote sites has been characterizing the site properties with a series of techniques.<sup>5-8</sup>

Lloyd *et al.*(2002)<sup>9</sup> specifically identified extrasolar planet detection via narrow angle astrometry as a being a unique niche available from Antarctic plateau sites. In this paper we update and extend that analysis to characterize the South Pole as a site for extrasolar planet science with an interferometer.

Further author information: (Send correspondence to J.P.L.)

J.P.L.: E-mail: jpl@astro.caltech.edu, Telephone: 1 626 395 8495

## 2. TURBULENCE THEORY

The optical significance of turbulence in the atmosphere is due to refractive index fluctuations, driven by temperature fluctuations. These temperature fluctuations are usually described in terms of a Kolmogorov model, with a temperature structure function as follows:

$$D_T(r) = \langle (T(x) - T(x+r))^2 \rangle = C_T^2 r^{2/3}.$$

Here,  $T$  is the temperature,  $x$  and  $r$  are location variables, and  $C_T^2$  characterizes the amplitude of the turbulence. These temperature fluctuations cause refractive index ( $N$ ) fluctuations through the refractivity dependence of air on temperature,  $C_N^2 = (\delta N / \delta T)^2 C_T^2$ .

The optical effect is characterized by the three-dimensional refractivity power spectrum, which for Kolmogorov turbulence is

$$\Phi(\kappa, h) = 0.033 C_N^2(h) \kappa^{-11/3}.$$

Here,  $\kappa$  is the spatial frequency of the turbulence, and  $C_N^2(h)$  describes the vertical profile, where  $h$  is the height above the observatory.  $C_N^2(h)$  is typically complicated, with multiple layers resulting from wind shear in the atmosphere.

The Fried parameter,  $r_0$ , relates the seeing to the equations above, and is the scale over which the height-integrated phase fluctuation at a given wavenumber,  $k = 2\pi/\lambda$ , equals one radian RMS.

Given a  $C_N^2(h)$  profile, the Fried parameter is

$$r_0 = \left[ 0.423 k^2 \sec(z) \int C_N^2(h) dh \right]^{-3/5},$$

and the FWHM of an image is  $0.98\lambda/r_0$ .  $z$  is the zenith angle of observation. For the rest of this paper, we will refer all calculations to the zenith. Thus, the integrated amplitude of  $C_N^2$  determines  $r_0$  and therefore the seeing. The integrated seeing to ice level has proven to be a major drawback for Antarctic telescopes, where the seeing is one to three arcseconds at  $0.5 \mu\text{m}$ , a value more typical of poor, low-altitude sites than superb sites such as Mauna Kea or Cerro Paranal, where the seeing is routinely below an arcsecond.

For any application that adaptively tracks the atmospheric phase fluctuations (e.g. adaptive optics, interferometry), the coherence time is a critical parameter. Coherence time can be defined in many ways.<sup>10</sup> Single layer, frozen flow approximation coherence times, assuming a phase screen with Fried parameter  $r_0$  moving at a wind speed  $V$  are common. This approximation may not be a good one considering the mechanisms that generate turbulence at the South Pole. The SODAR yields the full 3-D windspeed and  $C_N^2$  structure, so a single layer approximation is not required. For this paper, we adopt the definition based on the adaptive optics Greenwood frequency,<sup>11</sup> such that the servo bandwidth error is given by

$$\sigma_{BW}^2 = \kappa \left( \frac{f_G}{f_S} \right)^{5/3}$$

where

$$f_G = \left[ 0.102 k^2 \sec(z) \int_0^\infty C_N^2(h) v^{5/3}(h) dh \right]^{3/5}$$

and  $f_S$  is the closed loop servo bandwidth. This definition takes the correct account of any possible correlations between the wind speed and turbulence strength. For this paper, we calculate a two aperture coherence time  $T_{0,2} = 1/f_{G,2}$  from the single aperture Greenwood frequency above following Colavita *et al.* (1999).<sup>12</sup>

Other parameters, such as scintillation, isoplanatic angle, and tilt anisoplanatism, which have paramount significance in certain kinds of astronomical observations, depend on higher order moments of the  $C_N^2$  profile. Specifically, tilt anisoplanatism is the limiting error term for astrometric interferometry, and is a result of

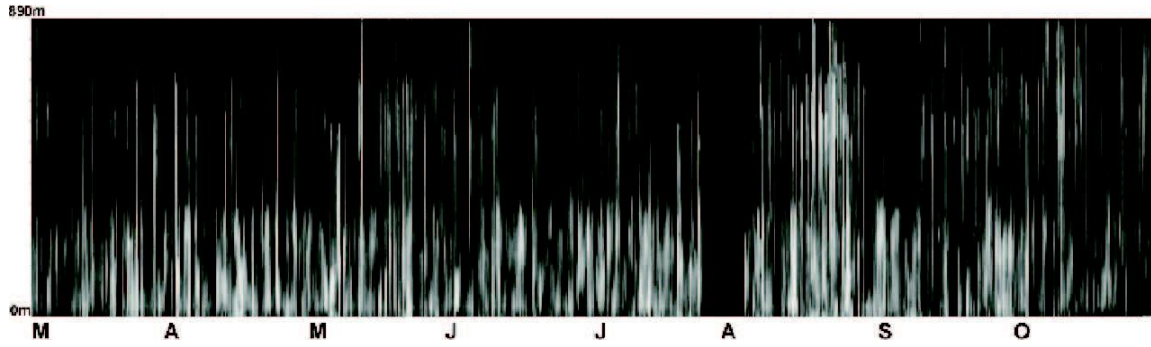


**Figure 1.** SODAR profiles throughout the 2000 Austral winter, between 2000 March and November (the letters on the x-axis mark the beginning of the month). The y-axis shows altitude from 0 to 890 meters while the brightness intensity shows the turbulence intensity. The turbulence intensity drops sharply between 200 and 400 meters, defining the boundary layer height.

the second moment of the  $C_N^2$  profile. The mean square error for an astrometric measurement with a dual-beam, differential astrometric interferometer in the very narrow-angle regime ( $\theta h \ll B$ ) with long integrations,  $t \gg B/V$ , is<sup>13</sup>:

$$\sigma_\delta^2 = 5.25 B^{-4/3} \theta^2 \int h^2 C_N^2(h) (Vt)^{-1} dh.$$

In this equation,  $B$  is the baseline of the interferometer,  $\theta$  is the angular separation of the celestial objects,  $V$  is the wind speed as a function of height, and  $t$  is total integration time of the observation. This calculation assumes a Kolmogorov power spectrum with no outer scale. Due to the  $h^2$  factor, this integral is completely dominated by high altitude turbulence. Thus, a site where the  $C_N^2$  profile is devoid of high altitude turbulence provides a substantial advantage.

### 3. SODAR PROFILES

Of particular interest here is the SODAR experiment to profile the lower 1km of the turbulence<sup>14</sup> as part of the Automated Astronomical Site Testing Observatory (AASTO) at the South Pole.

The SODAR used was a monostatic SODAR model PA1 manufactured by Remtech. Its antenna, placed on top of the AASTO, emits a series of 0.20 second long pulses at 5 different frequencies. The antenna then switches itself to receiving mode and records the echo pattern. This routine is repeated for an averaging period of 20 min, including sequences without emission that are used to calculate the background noise. After the averaging, the SODAR returns the echo strength which is proportional to  $C_T^2$ . The wind speed is derived from the Doppler shift of the returned echoes; the vertical component from the vertical beam and the horizontal components from the beams slanted at to the vertical. As previous studies have shown that the majority of the turbulence was concentrated in the lowest 300 m of the atmosphere, the SODAR was configured to make measurements from 20 m to 890 m with 30 m increments. The SODAR experiment, and the  $C_N^2$  profile results are discussed in detail in Travouillon *et al.*(2003).<sup>14</sup>

The primary limitation of the SODAR for completely characterizing the atmospheric turbulence is the limitation to altitudes below 890m. Since the  $C_N^2$  profile drops below the limiting sensitivity of the SODAR ( $2.6 \times 10^{-18} \text{m}^{-2/3}$ ) below this altitude, we assume for the purposes of this analysis that the SODAR profile is a complete description of the turbulence. While this is almost certainly incorrect in detail, since any turbulence below the sensitivity or above the altitude range is assumed to be zero, it provides a useful and concrete set of results about what has been measured, rather than surmised.

This assumption can be compared to differential image motion results from the ADIMM experiment<sup>15</sup> and the balloon microthermal results.<sup>3,4</sup> The ADIMM results (see Fig 3) are essentially consistent with the SODAR results (see Fig 2), indicating that there is no strong turbulence component at high altitude, as verified by

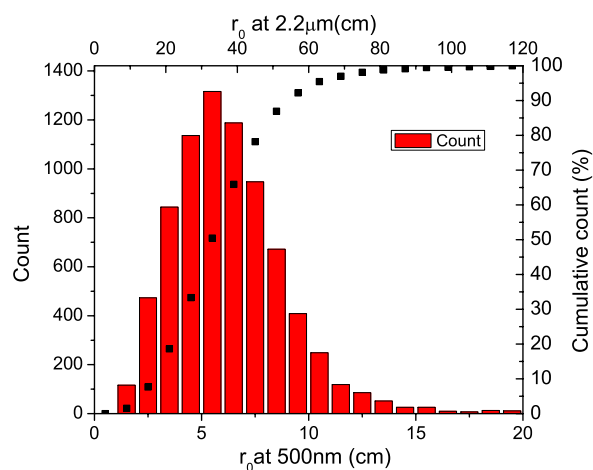


**Figure 2.** Fried parameter,  $r_0$  at 500 nm and  $2.2 \mu\text{m}$  as measured by the SODAR in 2000.

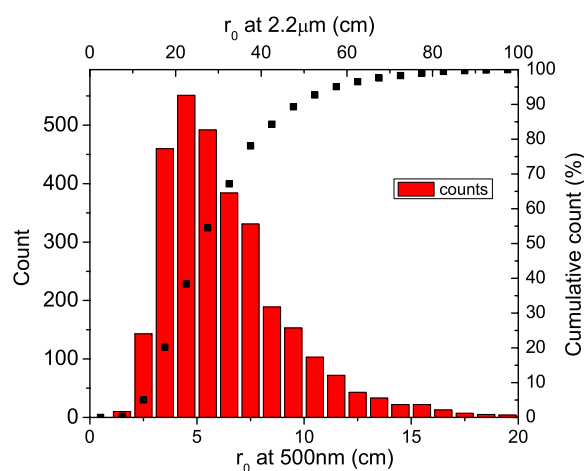


**Figure 3.** Fried parameter,  $r_0$  at 500 nm and  $2.2 \mu\text{m}$  as measured by the ADIMM in 2001.

the balloon flights. As the atmosphere above the boundary layer is nearly adiabatic, even in the presence of instabilities or turbulent velocity fields, the optical effect is minimized. Particularly given the lack of any evidence to indicate that any mechanism is in operation to generate turbulence at high altitude in the antarctic winter (e.g. jetstream or stratospheric heating), we will proceed with this assumption.

#### 4. DISCUSSION

The median  $r_0$  measured by the SODAR, 6 cm at 500 nm is relatively poor compared to good mid latitude sites, by a factor of 2-3. The distribution of coherence time at the South Pole is comparable to the measured  $T_{0,2}$  measured at Palomar with PTI,<sup>16</sup> although the PTI dataset is a selection of 64 nights, and the South Pole dataset is continuously recorded, regardless of observing conditions. The long coherence time tail is highly attractive as it can more than make up for the relatively poor  $r_0$ , which when combined with the low atmospheric emission yields a comparable sensitivity to a mid-latitude site, but with smaller required apertures. Differential Phase

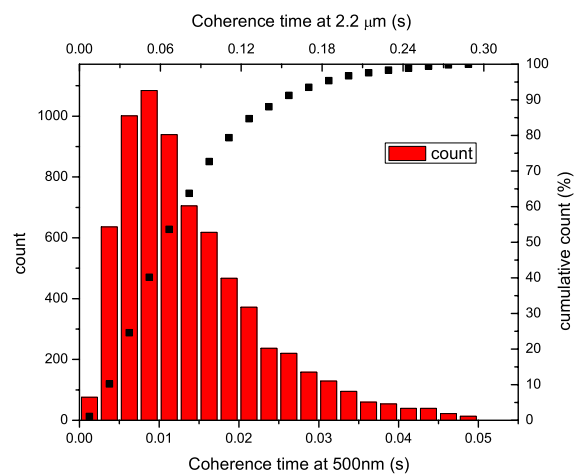


**Figure 4.** Coherence time,  $T_{0,2}$  at 500 nm and 2.2  $\mu\text{m}$  as measured by the SODAR in 2000.

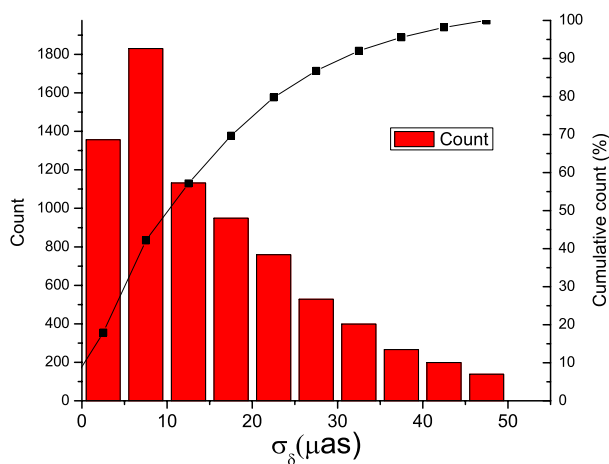


**Figure 5.** Astrometric error,  $\sigma_\delta$  (1 hr, 100m baseline,  $\theta = 1$  arcmin) as measured by the SODAR in 2000. The reference Mauna Kea atmosphere used in Shao and Colavita (1992) delivers 64  $\mu\text{as}$  with the same parameters.

is particularly attractive to attempt from the Antarctic Plateau as the cold dry air will avoid the systematic problem of water vapor fluctuations experienced at Mauna Kea.<sup>17</sup>

On the basis of these results, the largest gains are to be achieved in narrow angle astrometry. The large gain in coherence over angular separation can be put to use to achieve more precise astrometry or wider fields for phase reference calibrators, which is generally useful for all modes of phase referenced interferometry. Astrometric observations with accuracies near a few  $\mu\text{as}$  permit the detection and determination of the orbits of extrasolar planets. For reference, if a star like the Sun, lying at a distance of 10 pc, has a Jupiter-like planet orbiting it, the star's position will be perturbed by a maximum of 1 mas over the orbital period ( $\sim 12$  years). The signature of an Earth-like planet is approximately 1  $\mu\text{as}$ . Because a South Pole interferometer could, in principal, conduct observations indefinitely, within 10 years one could not only survey and determine the three dimensional orbital characteristics of the planets discovered through radial velocity studies, but also survey a substantial number of other stars within 30 pc for signatures of extrasolar planets. By comparison, the Space Interferometry Mission (SIM), which has a limited lifetime of 5 years, will be unable to observe stars over such long periods, limiting the types of planets it will find. It is necessary to fit the mass, semi-major axis, eccentricity, parallax and proper motion of the star in the astrometric solution. Accurate determination of all of these parameters with less than a complete orbit is not possible. It will therefore require significantly longer temporal baselines than SIM can provide to fully characterize the distribution of planets.

There are two substantial uncertain assumptions underlying these calculations. Firstly, as previously discussed, there is the question of unsensed component of the atmosphere. This will require additional experiments, particularly with sensitivity to high altitude components of turbulence. Secondly, the validity of the assumption of Kolmogorov turbulence is questionable. Once the interferometer baseline exceeds the outer scale of the turbulence, the dependence of  $\sigma_\delta$  no longer depends on  $B^{-2/3}$ . Inside the Kolmogorov regime, as the interferometer baseline increases, the additional power in on larger scales partially counteracts the improved resolution. Beyond the outer scale, the accuracy improves linearly with baseline as the phase fluctuation amplitude has saturated. There is strong evidence that the mechanism that generates the turbulence at the South Pole is Kelvin-Helmholtz instabilities in the wind shear of the inverted atmosphere. Waves in the cold, dense air in contact with the ice level are whipped up by the katabatic wind flow. When these waves break, turbulence is generated. This would explain the correlation between vertical wind speed and  $C_T^2$  observed in the SODAR data.<sup>14</sup> If this is the case, the turbulence is not generated by a cascade from large to small scales as is assumed in the Kolmogorov theory. If the turbulence is confined to a two dimensional layer the result will be a shallower Kolmogorov index. In general, the assumption of the turbulent cascade proceeding from large to small scales does not necessarily proceed in two dimensional turbulence, which can exhibit an "inverse cascade".<sup>18</sup> One might imagine that the outer scale would be confined to the thickness of the layer in which the turbulence is generated. The outer scale may therefore be exceptionally small, which would drastically alter the astrometric error results to much smaller values, below 1  $\mu\text{as hr}^{-1/2}$ . Measurements of the outer scale are therefore crucial to the ability to accurately predict the performance of an interferometer.

Finally, the South Pole is a site of convenience since there is a pre-existing station. There are strong arguments that sites with lower ground wind speed, such as Dome Concordia will offer even larger advantages since less turbulence will be generated, in a more confined boundary layer.

## ACKNOWLEDGMENTS

This work has been supported in part by the National Science Foundation Science and Technology Center for Adaptive Optics, managed by the University of California at Santa Cruz under cooperative agreement No. AST-9876783.

## REFERENCES

1. P. Gillingham, "Super seeing from antarctica," in *Optics in Astronomy: 32nd Herstmonceux Conference*, pp. 244+, 1993.
2. R. F. Loewenstein, C. Bero, J. P. Lloyd, F. Mrozek, J. Bally, and D. Theil, "Astronomical Seeing at the South Pole," in *ASP Conf. Ser. 141: Astrophysics From Antarctica*, pp. 296—, 1998.

3. R. D. Marks, J. Vernin, M. Azouit, J. F. Manigault, and C. Clevelin, "Measurement of optical seeing on the high antarctic plateau," *A&AS* **134**, pp. 161–172, Jan. 1999.
4. R. D. Marks, J. Vernin, M. Azouit, J. W. Briggs, M. G. Burton, M. C. B. Ashley, and J. F. Manigault, "Antarctic site testing - microthermal measurements of surface-layer seeing at the south pole.," *A&AS* **118**, pp. 385–390, Aug. 1996.
5. J. W. V. Storey, M. C. B. Ashley, and M. G. Burton, "An automated astrophysical observatory for Antarctica," *Publications of the Astronomical Society of Australia* **13**, pp. 35–38, Jan. 1996.
6. J. W. V. Storey, "The AASTO Program," in *ASP Conf. Ser. 141: Astrophysics From Antarctica*, pp. 313–+, 1998.
7. J. W. Storey, M. C. Ashley, and M. G. Burton, "Novel instruments for site characterization," in *Proc. SPIE Vol. 4008, p. 1376-1382, Optical and IR Telescope Instrumentation and Detectors*, Masanori Iye; Alan F. Moorwood; Eds., pp. 1376–1382, Aug. 2000.
8. J. Storey, M. Ashley, and M. Burton, "Antarctic Site Testing," in *ASP Conf. Ser. 266: Astronomical Site Evaluation in the Visible and Radio Range*, pp. 524–+, 2002.
9. J. P. Lloyd, B. R. Oppenheimer, and J. R. Graham, "The Potential of Differential Astrometric Interferometry from the High Antarctic Plateau," *Publications of the Astronomical Society of Australia* **19**, pp. 318–322, 2002.
10. D. F. Buscher, "A thousand and one nights of seeing on Mt. Wilson," in *Proc. SPIE Vol. 2200, p. 260-271, Amplitude and Intensity Spatial Interferometry II*, James B. Breckinridge; Ed., pp. 260–271, June 1994.
11. D. P. Greenwood, "Bandwidth specification for adaptive optics systems," *Optical Society of America Journal* **67**, pp. 390–393, Mar. 1977.
12. M. M. Colavita, J. K. Wallace, B. E. Hines, Y. Gursel, F. Malbet, D. L. Palmer, X. P. Pan, M. Shao, J. W. Yu, A. F. Boden, P. J. Dumont, J. Gubler, C. D. Koresko, S. R. Kulkarni, B. F. Lane, D. W. Mobley, and G. T. van Belle, "The Palomar Testbed Interferometer," *ApJ* **510**, pp. 505–521, Jan. 1999.
13. M. Shao and M. M. Colavita, "Potential of long-baseline infrared interferometry for narrow-angle astrometry," *A&A* **262**, pp. 353–358, Aug. 1992.
14. T. Travouillon, M. C. B. Ashley, M. G. Burton, J. W. V. Storey, and R. F. Loewenstein, "Atmospheric turbulence at the South Pole and its implications for astronomy," *A&A* **400**, pp. 1163–1172, Mar. 2003.
15. T. Travouillon, M. C. B. Ashley, M. G. Burton, P. G. Calisse, J. R. Everett, J. S. Lawrence, and J. W. V. Storey, "Some Antarctic Site Testing Results," in *SF2A-2002: Semaine de l'Astrophysique Francaise*, pp. 19–+, June 2002.
16. R. P. Linfield, M. M. Colavita, and B. F. Lane, "Atmospheric Turbulence Measurements with the Palomar Testbed Interferometer," *ApJ* **554**, pp. 505–513, June 2001.
17. R. L. Akeson, M. R. Swain, and M. M. Colavita, "Differential phase technique with the Keck Interferometer," in *Proc. SPIE Vol. 4006, p. 321-327, Interferometry in Optical Astronomy*, Pierre J. Lena; Andreas Quirrenbach; Eds., pp. 321–327, July 2000.
18. R. H. Kraichnan and D. Montgomery, "Two-dimensional turbulence," *Reports of Progress in Physics* **43**, pp. 547–619, May 1980.